ELSEVIER

Ceramics International 33 (2007) 447–452

CERAMICS INTERNATIONAL

www.elsevier.com/locate/ceramint

Electrical properties of $(1-x)(Bi_{0.5}Na_{0.5})TiO_3$–$xBaTiO_3$ synthesized by emulsion method

Bok-Hee Kim [a,*], Sang-Jae Han [a], Jong-Hwan Kim [a], Jeong-Hyung Lee [a], Byung-Kuk Ahn [a], Qing Xu [b]

[a] *Division of Advanced Materials Engineering, Research Institute of Advanced Materials Development, Chonbuk National University, Republic of Korea*

[b] *School of Material Science and Engineering, Wuhan University of Technology, China*

Received 19 September 2005; received in revised form 28 September 2005; accepted 27 October 2005

Available online 23 January 2006

Abstract

$(1-x)(Bi_{0.5}Na_{0.5})TiO_3$–$xBaTiO_3$ ($x = 0$–0.10)($(1-x)$BNT–xBT) powders were synthesized by a emulsion method, and the electrical properties of the resulting ceramics were investigated. The results confirm the emulsion method as a viable and advantageous route in producing $(1-x)$BNT–xBT ceramics. The powders consisting of uniform and fine preliminary particles of about 50 nm were synthesized by calcining at 700 °C for 3 h. The ceramics sintered at 1200 °C for 3 h show a rhombohedral–tetragonal morphotrophc phase boundary (MPB) near $x = 0.06$. The ceramics provide superior dielectric and piezoelectric properties close to the phase boundary. The dielectric constant at 1 kHz and piezoelectric constant d_{33} attain the maximum values of 1840 and 174 pC/N, respectively, at $x = 0.08$, while the electromechanical coupling factor k_p exhibits the maximum value of 0.28 at $x = 0.06$.

Keywords: Dielectric properties; Piezoelectric properties; $(1-x)(Bi_{0.5}Na_{0.5})TiO_3$–$xBaTiO_3$; Emulsion method

1. Introduction

Lead-containing ferroelectric materials such as $Pb(Zr,Ti)O_3$ (PZT) based ceramics have been widely used as ultrasonic transducers, sensors and actuators in various electronic devices because of their excellent piezoelectric properties. However, in spite of the superior properties, the lead-containing materials are restricted in using by many advanced countries because the toxicity of lead oxide causes an environmental pollution [1–3]. Recently, there are increasing interests in investigating lead-free materials with high dielectric and piezoelectric properties to replace the lead containing ferroelectrics. $Bi_{0.5}Na_{0.5}TiO_3$ (BNT) was found to be ferroelectric with a perovskite structure at room temperature in 1960 by Smolenskii et al. [4]. BNT is considered as one of promising lead-free piezoelectric materials due to a large remnant polarization ($P_r = 38$ μC/cm^2) at room temperature and a high Curie temperature ($T_c = 320$ °C). However, pure BNT ceramics is difficult to be fully poled owing to its high coercive field ($E_c = 73$ kV/cm), to be sintered and has relatively low piezoelectric properties. It has been found that the substitution at the A site of BNT with appropriate cations resulted in an improvement of sintering and piezoelectric properties [5–7].

BNT based compositions can be prepared by various methods. It is comparatively simple to synthesize BNT based compositions by the traditional solid state reaction process [8]. Nevertheless, when using this process, it is difficult to maintain chemical homogeneity of obtained powders because of heterogeneous reaction among solid powders of starting materials. Some recent researches have been devoted to the synthesis of BNT based powders by various wet chemical processes, such as co-precipitation process [9], sol–gel process [10] and hydrothermal method [11]. Emulsion method is a suitable route for preparing powders of multi-component systems [12–13]. In this work, $(1-x)(Bi_{0.5}Na_{0.5})TiO_3$–$xBaTiO_3$ ($x = 0$, 0.02, 0.04, 0.06, 0.08 and 0.10) powders were synthesized using the emulsion method. The dielectric and piezoelectric properties of the resulting ceramics were also investigated.

* Corresponding author. Tel.: +82 63 270 2380; fax: +82 63 270 2386.

0272-8842/$32.00
doi:10.1016/j.ceramint.2005.10.022

2. Experimental

Bi_2O_3 (99.0%, Junsei Chemical Co., Ltd. Japan), Na_2CO_3 (99.0%, Junsei Chemical Co., Ltd. Japan), $Ba(NO_3)_2$ (98.5%, Shinyo Pure Chemicals Co., Ltd. Japan) and $TiCl_4$ (99.9%, Aldrich Chemical Company, Inc., USA) were chosen as starting materials. These materials were dissolved into acidic solution according to the nominal composition of $(1-x)(Bi_{0.5}Na_{0.5})TiO_3$–$xBaTiO_3$ ($x = 0$, 0.02, 0.04, 0.06, 0.08 and 0.10) (abbreviated as $(1-x)$BNT–xBT thereafter), and then mixed on a magnetic stirrer for 24 h to prepare homogeneous mixed solution with a concentration 0.5 mol/L. With span 80 (5%, v/v) as surfactant, kerosene (92%, v/v) as solvent and paraffin oil (3%, v/v) as emulsifying agent, the organic phase for emulsifying was prepared by mixing on the magnetic stirrer for 24 h.

The homogeneous mixed solution and organic phase were mixed in a volume ratio of 2:1 and rotated at a speed of 4000 rpm for 5 min to form water-in-oil type emulsion. To evaporate the water included in the emulsion rapidly, the prepared emulsion was sprayed into the kerosene heated at 170 °C. Powder was derived from the emulsion after filtering and drying at 120 °C in an oven.

The emulsion-derived powders were calcined in the temperature range of 400–800 °C for 2–4 h in air at a heating and cooling rate of 5 °C/min. The calcined powders were pressed into discs of 13 mm in diameter and 1 mm in thickness under an uniaxial pressure of 1000 kg/cm^2. The compacted discs were sintered at 1150–1225 °C for 2–4 h in air at a heating and cooling rate of 5 °C/min.

Thermogravimetry (TG) and differential thermal analysis (DTA) of the emulsion-derived powders were carried out using a simultaneous thermal analyzer (TA Instruments, DSC 2920, TGA 2950) at a heating rate of 5 °C/min. The crystal structure of the emulsion-derived powders, calcined powders and sintered bodies was examined using an X-ray diffractometer (Rigaku, D/MAX-111A) with Cu Kα radiation operated at 40 kV, 30 mA and scanning speed of 4 °/min. The morphology of the emulsion-derived and calcined powders was observed using a field emission scanning electron microscope (Hitach, S-4700 in KBSI). The microstructure of ceramics was investigated with a scanning electron microscope (SEM, JEOL JSM-6400) using thermally etched surfaces. The relative density of the ceramics was measured by the Archimedes method. The ceramic specimens were painted with silver electrode on both surfaces and poled in a silicon oil bath at 60 °C for 10 min under a dc field of 3 kV/mm. The dielectric properties of the ceramics before poling were measured at 1 kHz using a HP 4194A impedance/gain-phase analyzer. The piezoelectric constant (d_{33}) was measured using a quasistatic d_{33} meter (Academia Sinica, ZJ-4B). The electromechanical coupling factor (k_p) was measured by the resonance-anti-resonance method using a HP 3577A network analyzer.

3. Results and discussion

As a terminal composition of $(1-x)$BNT–xBT solid solution, pure BNT was chosen as a representative to examine the optimum synthesis and sintering conditions of $(1-x)$BNT–xBT compositions.

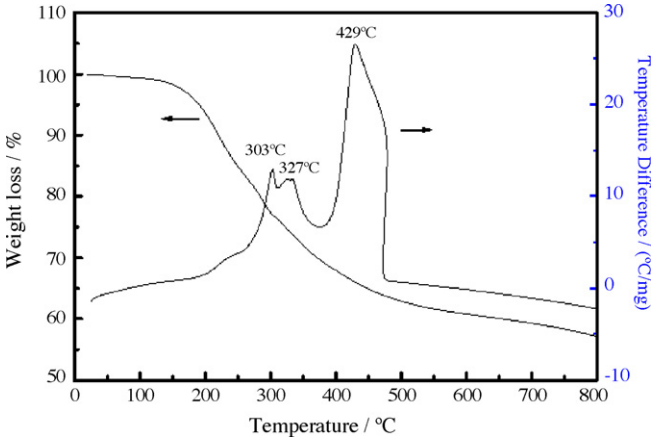

Fig. 1. DT–TGA curves of emulsion-dried BNT powder.

Fig. 1 shows the DT–TGA curves of emulsion-derived BNT powder. Three exothermic peaks at 303, 327 and 429 °C, respectively, were observed in the DTA curve, accompanied by an obvious gravity decrease within the corresponding temperature range in the TGA curve, which is attributed to the oxidation of the organic components and nitrates remained in the emulsion-derived powder. It was found that the thermal decomposition of the emulsion-derived powder was finished before 500 °C. Fig. 2 shows the X-ray diffraction (XRD) pattern of emulsion-derived BNT powder. The result indicates that only $NaNO_3$ was precipitated during drying the emulsion and other start materials exist in an amorphous state. Fig. 3 shows FE-SEM micrographs of emulsion-derived BNT powder under different magnifications. It can be seen that the emulsion-derived powder has a spherical morphology, formed by the agglomeration of preliminary particles of 20–30 nm. It is considered that the spherical shape is due to the surface energy of the emulsion and the nano-sized preliminary particles were generated during drying the colloid sized emulsion.

Fig. 4 shows the XRD patterns of BNT powders calcined at 400–800 °C for 3 h. BNT was formed at 400 °C as a main

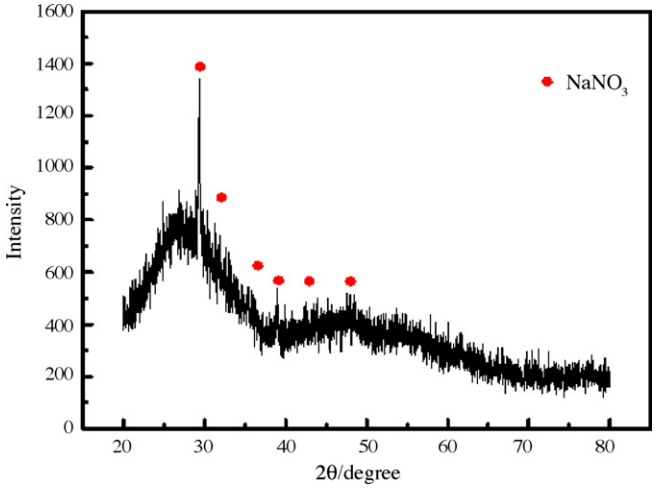

Fig. 2. XRD pattern of emulsion-derived BNT powder.

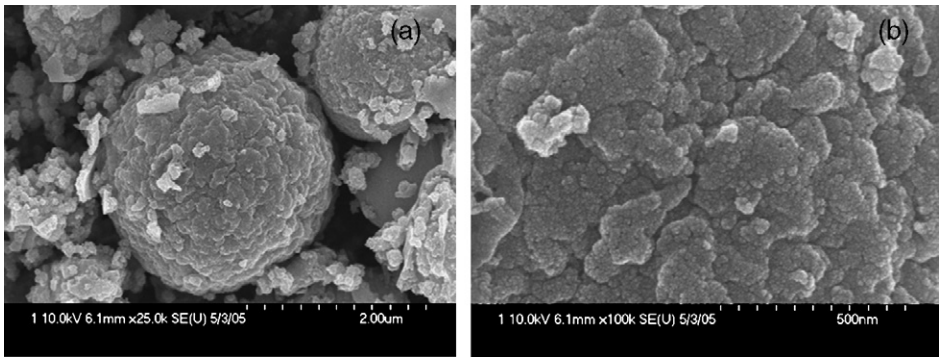

Fig. 3. FE-SEM micrographs of emulsion-derived BNT powder under magnifications of (a) 20 k and (b) 100 k.

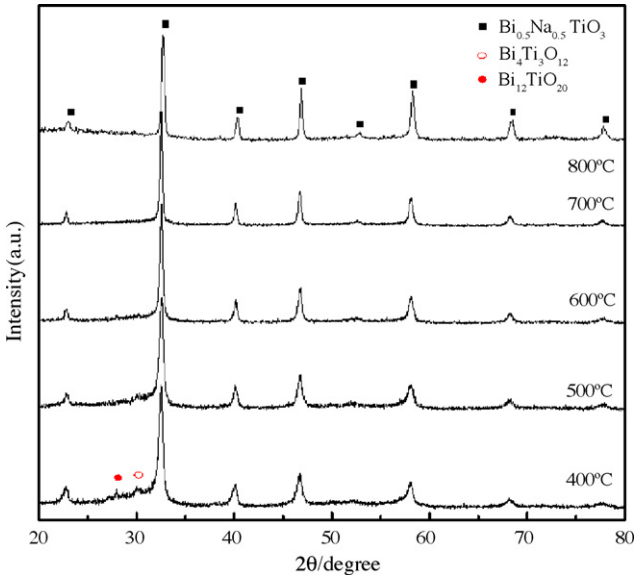

Fig. 4. XRD patterns of BNT powders calcined at different temperatures for 3 h.

crystal phase together with minor amounts of intermediate phases $Bi_{12}TiO_{20}$ and $Bi_4Ti_3O_{12}$. The intermediate phases still remain until 500 °C, and the further elevation of calcining temperature to 600 °C produced a single BNT phase. When using the tradition solid state reaction process, a single BNT phase is produced at about 900 °C [14]. By comparison, a single BNT phase can be obtained at a relatively lower temperature of 600 °C by using the emulsion method.

BNT powders calcined under different conditions (calcining temperature and time) were sintered at 1200 °C for 3 h. The relative densities of these ceramics are shown in Fig. 5. In Fig. 5(a), the powders were calcined at 500–800 °C for 3 h. The relative density attains the maximum value of 96.1% at the calcining temperature of 700 °C. In Fig. 5(b), the powders were calcined at 700 °C for 2–4 h, showing the maximum relative density at the calcining time of 3 h. Therefore, calcining at 700 °C for 3 h was determined to be preferred for BNT composition.

BNT powder calcined at 700 °C for 3 h was sintered under different conditions (sintering temperature and time). Fig. 6 shows the relative densities of these ceramics. The results indicate that it is preferred to sinter the ceramic at 1200 °C for 3 h in order to obtain the maximum relative density. The decrease in the relative density of the ceramics sintered at a higher temperature (1225 °C) or for a longer time (4 h) is assumedly ascribed to an exaggerated evaporation of Na and Bi during sintering.

Thus, the optimum preparing conditions for BNT ceramic can be ascertained as calcining at 700 °C for 3 h and then sintering at 1200 °C for 3 h. These optimum preparing conditions were applied for other $(1 - x)$BNT–xBT compositions. Fig. 7 shows the FE-SEM micrograph of BNT powder calcined at 700 °C for 3 h and SEM micrograph of the resulting ceramic sintered at

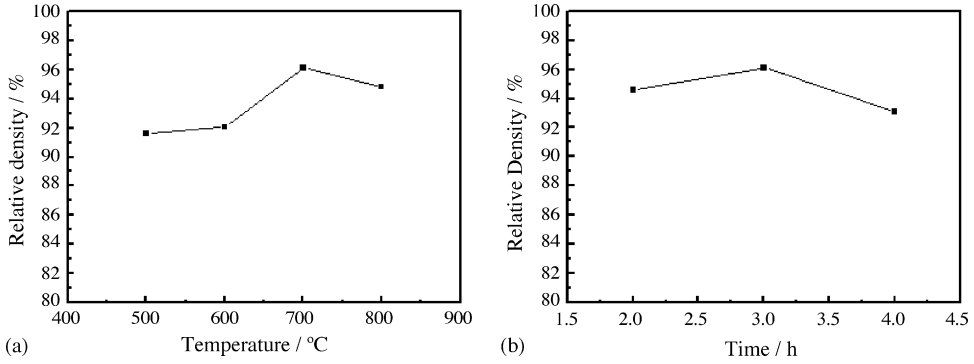

Fig. 5. Relative densities of BNT ceramics made from powders calcined (a) at various temperatures for 3 h and (b) at 700 °C for various times. The ceramics were sintered at 1200 °C for 3 h.

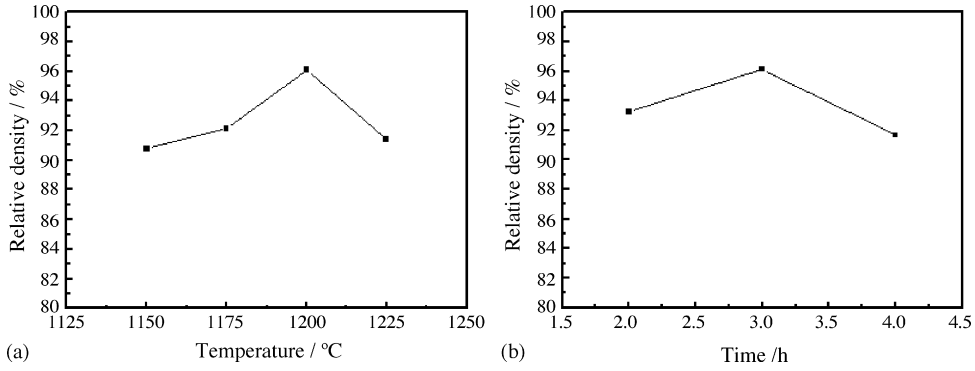

Fig. 6. Relative densities of BNT ceramics sintered (a) at various temperatures for 3 h and (b) at 1200 °C for various times. The powders were calcined at 700 °C for 3 h.

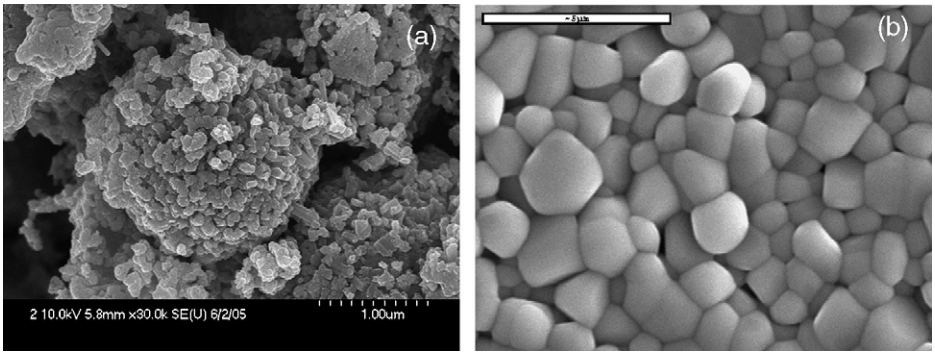

Fig. 7. (a) FE-SEM micrograph of BNT powder calcined at 700 °C for 3 h and (b) SEM micrograph of BNT ceramic sintered at 1200 °C for 3 h.

1200 °C for 3 h. Compared with the morphology of the emulsion-derived powder (Fig. 3), the calcined powder has a comparatively porous morphology, showing an aggregation of fine and uniform preliminary particles of about 50 nm (Fig. 7(a)). This is believed to be caused by the release of gases during the calcination. The resulting ceramic shows a dense microstructure with grain sizes of 1–2.5 μm (Fig. 7(b)). The dense microstructure can be attributed to the homogeneous and fine morphology of preliminary particles in the calcined powder. Similar results were also obtained from the calcined powders and ceramics of other $(1-x)$BNT–xBT compositions.

Fig. 8 shows the XRD patterns of $(1-x)$BNT–xBT ceramics. Fig. 8(a) identifies the formation of a single perovskite structure for the ceramics. Fig. 8(b) shows the XRD patterns of the ceramics in the 2θ range of 38–48°. The rhombohedral symmetry of BNT ceramic at room temperature can be characterized by a (0 0 3)/(0 2 1) peak splitting between 39 and 41° and a single peak of (2 0 2) between 45 and 48°. The rhombohedral (0 0 3)/(0 2 1) peak splitting is remained until $x = 0.06$ and then combines into a slightly asymmetric peak at $x = 0.08$. On the other hand, the (2 0 2) peak became broad and asymmetric at $x = 0.04$. A distinct (0 0 2)/(2 0 0) peak splitting

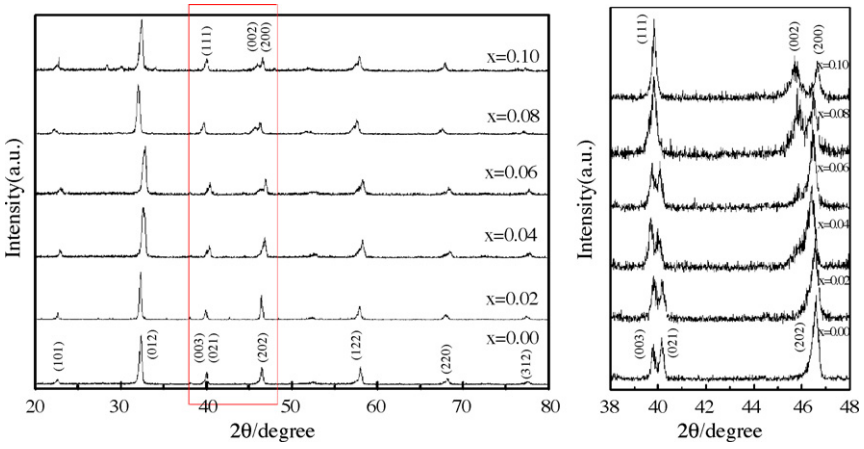

Fig. 8. XRD patterns of $(1-x)$BNT–xBT ceramics sintered at 1200 °C for 3 h.

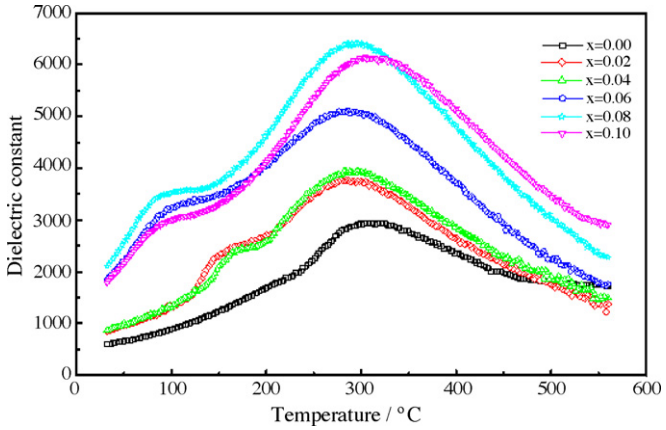

Fig. 9. Dielectric constant of $(1-x)$BNT–xBT ceramics as a function of temperature measured on cooling.

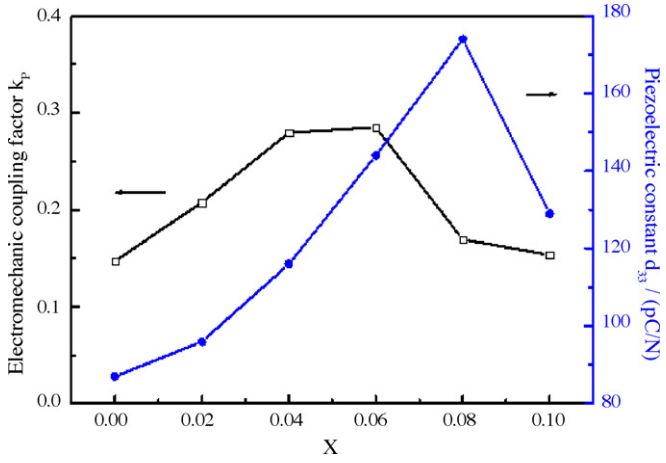

Fig. 10. Piezoelectric properties of $(1-x)$BNT–xBT ceramics.

appears when $x \geq 0.06$, referring to a tetragonal symmetry. These results suggest that the rhombohedral–tetragonal morphotrophc phase boundary (MPB) of $(1-x)$BNT–xBT ceramics is near $x = 0.06$. It is consistent with an early result obtained from $(1-x)$BNT–xBT ceramics prepared by the traditional solid state reaction process [15].

Fig. 9 shows the dielectric constant of $(1-x)$BNT–xBT ceramics as a function of temperature measured on cooling. The dielectric constant at room temperature attains the maximum value of 1840 at $x = 0.08$, which is in agreement with the nature of this specimen with a composition near the MPB. For pure BNT, an obscure hump in the variation of dielectric constant with temperature occurred near 200 °C, corresponding to a ferroelectric (rhombohedral)–antiferroelectric (tetragonal) phase transition [16]. Other $(1-x)$BNT–xBT ceramics display a comparatively obvious ferroelectric–antiferroelectric phase transition. It was noticed that increasing BT content resulted in a decrease of the transition temperature.

Fig. 10 shows the piezoelectric properties of $(1-x)$BNT–xBT ceramics. The ceramics provide superior piezoelectric properties near the MPB, with the electromechanical coupling factor k_p and piezoelectric constant d_{33} exhibiting the maximum values of 0.28 and 174 pC/N at $x = 0.06$ and 0.08, respectively. It has been reported that the piezoelectric constant and electromechanical coupling factor of $(1-x)$BNT–xBT ceramics prepared by the traditional solid state method reach maximum values of $d_{33} = 122$ pC/N and $k_p = 0.29$ near the MPB [15]. The maximum value of electromechanical coupling factor k_p in the present work is compatible with the early reported result, while that of piezoelectric constant d_{33} is much more larger. This demonstrates the advantage of the emulsion method in improving the piezoelectric properties of $(1-x)$BNT–xBT ceramics. It is presumably assigned to the homogeneity in the morphology and composition of preliminary particles of the powders synthesized by the emulsion method.

4. Conclusion

This research confirms that the emulsion method is an advantageous alternative to the traditional solid state reaction process in producing lead free $(1-x)(Bi_{0.5}Na_{0.5})TiO_3$–$xBaTiO_3$ ($(1-x)$BNT–xBT) ceramics. The optimum preparing conditions for $(1-x)$BNT–xBT ceramics were ascertained in terms of relative density of the ceramics. The powders consisting of uniform and fine preliminary particles of about 50 nm can be yielded by calcining at 700 °C for 3 h. The ceramics sintered at 1200 °C for 3 h show a rhombohedral–tetragonal morphotrophc phase boundary (MPB) near $x = 0.06$. The ceramics present high dielectric and piezoelectric properties near the MPB. The dielectric constant at 1 kHz and piezoelectric constant d_{33} attain the maximum values of 1840 and 174 pC/N, respectively, at $x = 0.08$, while the electromechanical coupling factor k_p gives the maximum value of 0.28 at $x = 0.06$.

Acknowledgements

It is grateful to Korea Science and Engineering Foundation (Grant No. F01-2004-000-10084-0) and Natural Science Foundation of China (Grant No. 50272044 and 50411140529) for jointly supporting the research. This research was also supported by the Program for the Training of Graduate Students in Regional Innovation which was conducted by the Ministry of Commerce Industry and Energy of the Korean Government.

References

[1] H.C. Wang, W.A. Sculze, The role of excess magnesium oxide or lead oxide in determining the microstructure and properties of lead magnesium niobate, J. Am. Ceram. Soc. 73 (4) (1990) 825–832.
[2] L.F. Francis, D.A. Payne, Thin-layer dielectrics in the $Pb[(Mg_{1/3}Nb_{2/3})1-xTi_x]O_3$ system, J. Am. Ceram. Soc. 74 (12) (1991) 3000–3010.
[3] S.H. Cho, J.V. Biggers, Characterization and sintering of lead zirconate–titanate powders, J. Am. Ceram. Soc. 66 (10) (1983) 743–746.
[4] G.A. Smolensky, V.A. Isupov, R.I. Agranovskaya, N.N. Kainik, New ferroelectrics of complex composition, Sov. Phys. Solid State 2 (1961) 2651–2654.
[5] J. Suchanicz, J. Kusz, H. Boehm, H. Duda, J.P. Mercurio, K. Konieczny, Structural and dielectrics of $(Na_{0.5}Bi_{0.5})_{0.70}Ba_{0.30}TiO_3$ ceramics, J. Eur. Ceram. Soc. 23 (2003) 1559–1564.
[6] X. Wang, H.L. Chan, C. Choy, Piezoelectric and dielectric properties of CeO_2-added $(Bi_{0.5}Na_{0.5})_{0.94}Ba_{0.06}TiO_3$ lead-free ceramics, Solid State Commun. 125 (2003) 395–399.

[7] A. Herabut, A. Safari, Processing and electromechanical properties of $(Bi_{0.5}Na_{0.5})_{(1-1.5x)}La_xTiO_3$ ceramics, J. Am. Ceram. Soc. 80 (1997) 2954–2958.

[8] H. Nagata, T. Takenaka, Additive effects on electrical properties of $(Bi_{1/2}Na_{1/2})TiO_3$ ferroelectric ceramics, J. Eur. Ceram. Soc. 21 (2001) 1299–1302.

[9] A.Q. Jiang, G.H. Li, L.D. Zhang, Absorption red shift and structural phase transition in nanocrystalline $Bi_4Ti_3O_{12}$–Na_2TiO_3 solid solution, Solid State Commun. 104 (1997) 709–711.

[10] S. Said, J.P. Mercurio, Relaxor behaviour of low lead free ferroelectric ceramics of the $Na_{0.5}Bi_{0.5}TiO_3$–$PbTiO_3$ and $Na_{0.5}Bi_{0.5}TiO_3$–$K_{0.5}Bi_{0.5}TiO_3$ systems, J. Eur. Ceram. Soc. 21 (2001) 1333–1336.

[11] M.M. Lencka, M. Oledzka, R.E. Riman, Hydrothermal synthesis of sodium and potassium bismuth titanates, Chem. Mater. 12 (2000) 1323–1330.

[12] Bok-Hee Kim, Ji-Won Moon, Jo-Young Lee, Youn-Kyu Choi, Synthesis of perovskite $Pb(Mg_{1/3}Nb_{2/3})O_3$ powder by emulsion method, J. Ceram. Soc. Jpn. 107 (2) (1999) 115–118.

[13] Bok-Hee Kim, Youn-Kyu Choi, Yong-Ho Choa, Synthesis of $LiFe_xMn_{2-x}O_4$ cathode materials by emulsion method and their electrochemical properties, Solid State Ionics 158 (2003) 281–285.

[14] Y. Lin, S. Zhao, N. Cai, J. Wu, X. Zhou, C.W. Nan, Effects of doping Eu_2O_3 on the phase transformation and piezoelectric properties of $Na_{0.5}Bi_{0.5}TiO_3$-based ceramics, Mat. Sci. Eng. B 99 (2003) 449–452.

[15] B.-J. Chu, D.-R. Chen, G.-R. Li, Q.-R. Yin, Effect of A-site substitution on crystal component and dielectric properties in $Bi_{0.5}Na_{0.5}TiO_3$ ceramics, J. Eur. Ceram. Soc. 22 (2002) 2115–2121.

[16] Y. Qu, D. Shan, J. Song, Electrical properties of $Na_{1/2}Bi_{1/2}TiO_3$–$BaTiO_3$ ceramics, Mat. Sci. Eng. B 121 (2005) 148–151.